4. Approximation in Line Space

4.1 Fitting Linear Complexes

The applications of the concept of linear line complex discussed in Sec. 3.4 show that it is important to study the problem of approximation of and with linear complexes. We consider the following questions: which linear complex fits a given set of data lines best? What is an appropriate definition of 'best' for various applications? For this we have to define distance functions for lines and linear complexes, which make the problem computationally tractable. It turns out that most approximation problems can be accessed by least-square methods.

The Moment of a Line with respect to a Linear Complex

Consider Euclidean three-dimensional space E^3, a line L and a linear complex $\mathcal{C}$. Assume that their homogeneous Plücker coordinates are $(\mathbf{l}, \bar{\mathbf{l}})$ and $(\mathbf{c}, \bar{\mathbf{c}})$, respectively, with $\mathbf{c} \neq \mathbf{o}, \mathbf{l} \neq \mathbf{o}$ (i.e., L is not an ideal line, and $\mathcal{C}$ is not the path normal complex of a translation). The following definition was given by F. Klein:

Definition. *Under the assumptions above, the moment of the line L with respect to the linear complex $\mathcal{C}$ is defined by*

$$m(L, \mathcal{C}) = \frac{1}{\|\mathbf{c}\| \, \|\mathbf{l}\|} |\bar{\mathbf{c}} \cdot \mathbf{l} + \mathbf{c} \cdot \bar{\mathbf{l}}| = \frac{1}{\|\mathbf{c}\| \, \|\mathbf{l}\|} |\Omega((\mathbf{c}, \bar{\mathbf{c}}), (\mathbf{l}, \bar{\mathbf{l}}))|. \tag{4.1}$$

If we use *normalized* Plücker coordinates for L and $\mathcal{C}$, which means $\|\mathbf{l}\| = \|\mathbf{c}\| = 1$, then (4.1) becomes $m(L, \mathcal{C}) = |\Omega((\mathbf{c}, \bar{\mathbf{c}}), (\mathbf{l}, \bar{\mathbf{l}}))|$.

Remark 4.1.1. As we did with lines, we can assign two *oriented* linear complexes to a linear complex $\mathcal{C}$. If $\mathcal{C}$ has Plücker coordinates $(\mathbf{c}, \bar{\mathbf{c}})$ with $\mathbf{c} \neq \mathbf{o}$, there are two ways to normalize the vector $\mathbf{c}$. Any of the coordinate six-tuples $\pm(1/\|\mathbf{c}\|)(\mathbf{c}, \bar{\mathbf{c}})$ is called an oriented linear complex $\vec{\mathcal{C}}$ belonging to $\mathcal{C}$.

If $\vec{\mathcal{C}} = (\mathbf{c}, \bar{\mathbf{c}})$ with $\|\mathbf{c}\| = 1$, and the line L has the normalized Plücker coordinates $(\mathbf{l}, \bar{\mathbf{l}})$, we let $m(\vec{L}, \vec{\mathcal{C}}) = \Omega((\mathbf{c}, \bar{\mathbf{c}}), (\mathbf{l}, \bar{\mathbf{l}}))$, and call this value the moment of the oriented line $\vec{L}$ with respect to $\vec{\mathcal{C}}$.

Lemma 3.4.11 shows that $m(\vec{L}, \vec{\mathcal{C}})$ has an interpretation as a virtual work. We will not need the moments of oriented lines and complexes, and we will always use Equ. (4.1), which defines $m(L, \mathcal{C})$ to be nonnegative. ◇

H. Pottmann and J. Wallner, *Computational Line Geometry*,
Mathematics and Visualization, DOI 10.1007/978-3-642-04018-4_4,

We are interested in the set of lines whose moment with respect to the linear complex $\mathcal{C}$ equals a certain constant. This set has the following geometric description:

Lemma 4.1.1. *Assume that L is a line and $\mathcal{C}$ is a linear complex of pitch p such that $m(L,\mathcal{C})$ is defined. If $P \in L$, r is P's distance to the axis A of $\mathcal{C}$ and α is the minimum of angles enclosed by L and a line of $\mathcal{C}$ incident with P, then*

$$m(L,\mathcal{C}) = \sqrt{r^2 + p^2}\sin\alpha. \tag{4.2}$$

Proof. The lines of $\mathcal{C}$ are path normals of the unique helical motion with pitch p and axis A. If T denotes the path tangent of P, then obviously $\pi/2 - \alpha = \sphericalangle(L,T)$. Without loss of generality, the helical motion has the form (3.6) and $\mathcal{C}$ therefore the equation (3.8). Now (4.2) follows by a simple computation. □

We see that the moment $m(L,\mathcal{C})$ vanishes if and only if $L \in \mathcal{C}$. The set $\mathcal{K}$ of lines such that $\sqrt{r^2 + p^2}\sin\alpha$ is constant (with the symbols used in Lemma 4.1.1) is called a *cyclic quadratic complex*. Its complex cones are right circular cones, and its complex curves are circles. We will discuss it in Sec. 7.2.3.

Deviation of a Linear Complex from a Set of Lines

We assume that lines $L_1, \ldots, L_k$ are given by their normalized Plücker coordinates $(\mathbf{l}_i, \bar{\mathbf{l}}_i)$ ($\|\mathbf{l}_i\| = 1$). It is fortunate that the moment of a line L_i with respect to a linear complex $\mathcal{X}$ is a bilinear form if we restrict ourselves to normalized Plücker coordinates. The sum of moments equals a quadratic function:

$$\sum_{i=1}^{k} m(L_i,\mathcal{X})^2 = F(\mathbf{x},\bar{\mathbf{x}}) = \sum_{i=1}^{k}(\bar{\mathbf{x}}\cdot\mathbf{l}_i + \mathbf{x}\cdot\bar{\mathbf{l}}_i)^2. \tag{4.3}$$

We use the expression (4.3) as a measure of the deviation of a linear complex $\mathcal{X}$ from the set $\{L_1, \ldots, L_k\}$ of lines. The function F is a positive semidefinite quadratic form defined in $\mathbb{R}^6$. To compute its coordinate matrix, we observe that the product $(\mathbf{a}\cdot\mathbf{b})(\mathbf{c}\cdot\mathbf{d})$ is in matrix notation written as $\mathbf{b}^T\cdot(\mathbf{a}\cdot\mathbf{c}^T)\cdot\mathbf{d}$. Thus we let

$$M = \sum_{i=1}^{k} \left(\begin{array}{c|c} \bar{\mathbf{l}}_i\cdot\bar{\mathbf{l}}_i^T & \mathbf{l}_i\cdot\bar{\mathbf{l}}_i^T \\ \hline \bar{\mathbf{l}}_i\cdot\mathbf{l}_i^T & \mathbf{l}_i\cdot\mathbf{l}_i^T \end{array}\right), \tag{4.4}$$

and we see that F can be expressed in the form

$$F(\mathbf{x},\bar{\mathbf{x}}) = (\mathbf{x},\bar{\mathbf{x}})^T\cdot M\cdot(\mathbf{x},\bar{\mathbf{x}}). \tag{4.5}$$

Computation of an Approximant Complex in the Regular Case

In order to compute a linear complex $\mathcal{X}$ which approximates the given set of lines $L_1, \ldots, L_k$, we look for normalized Plücker coordinates $(\mathbf{x},\bar{\mathbf{x}})$ which minimize

$F(\mathbf{x}, \overline{\mathbf{x}})$. This approximation problem makes sense only for $k \geq 5$, because otherwise there is at least a one-parameter family of linear complexes which contains all given lines. There is a unique linear complex which contains five lines in general position, so we we always assume that $k > 5$.

Lemma 4.1.2. *In the set of Plücker coordinate vectors* $(\mathbf{x}, \overline{\mathbf{x}})$ *with* $\|\mathbf{x}\| = 1$, *the function* F *of Equ. (4.3) attains its minimum* λ *precisely for those* $(\mathbf{x}, \overline{\mathbf{x}})$ *which fulfill*

$$(M - \lambda D) \cdot (\mathbf{x}, \overline{\mathbf{x}}) = \mathbf{o}, \quad \|\mathbf{x}\| = 1, \tag{4.6}$$

where $D = \operatorname{diag}(1, 1, 1, 0, 0, 0)$, M *is defined by (4.4), and* λ *is the smallest solution of the equation*

$$\det(M - \lambda D) = 0. \tag{4.7}$$

Proof. We have to minimize $F(\mathbf{x}, \overline{\mathbf{x}})$ subject to the side condition $G(\mathbf{x}, \overline{\mathbf{x}}) = \|\mathbf{x}\| = 1$. This side condition is expressed in matrix notation by $(\mathbf{x}, \overline{\mathbf{x}})^T \cdot D \cdot (\mathbf{x}, \overline{\mathbf{x}}) = 1$. We introduce the Lagrangian multiplier λ and solve $\operatorname{grad}_F(\mathbf{x}, \overline{\mathbf{x}}) - \lambda \operatorname{grad}_G(\mathbf{x}, \overline{\mathbf{x}}) = \mathbf{o}$, which simplifies to Equ. (4.6). A nonzero solution obviously is possible if and only if $M - \lambda D$ is singular.

Then $M \cdot (\mathbf{x}, \overline{\mathbf{x}}) = \lambda \cdot D \cdot (\mathbf{x}, \overline{\mathbf{x}})$, and Equ. (4.5) shows that $F(\mathbf{x}, \overline{\mathbf{x}}) = \lambda$. This shows that in order to minimize F we have to choose the smallest possible λ. □

Remark 4.1.2. The statistical standard deviation of the approximating linear complex $\mathcal{X}$ from the given lines equals

$$\sigma = \sqrt{\lambda/(k-5)}.$$

The smaller λ is, the better the solution complex fits the original data $L_1, \ldots, L_k$. 'Small' however has only a relative meaning. If the input data are scaled by a factor α, the value of λ scales with α^2. So σ, which scales linearly with the input data, and whose definition accounts for the number of input lines, should be compared with the size of objects under discussion. ◇

Complexes of Zero Pitch

If the pitch p of the approximant complex $\mathcal{C}$ turns out to be very small, one might be interested in fitting the input data by a singular linear complex $\mathcal{C}_0$ of zero pitch. By Th. 3.1.3, such a complex consists of all lines which intersect a line A_0. Thus we have to determine A_0 such that it 'almost' intersects the input lines $L_1, \ldots, L_k$.

The simplest choice is to take the axis of the approximant complex, computed by Equ. (3.9). We achieve a better result if we minimize within the set of singular complexes:

Lemma 4.1.3. *In the set of normalized Plücker coordinates* $(\mathbf{x}, \overline{\mathbf{x}})$ *of singular linear complexes (i.e.,* $\|\mathbf{x}\| = 1$, $\mathbf{x} \cdot \overline{\mathbf{x}} = 0$*), the function* F *of Equ. (4.3) attains its minimum* λ *for a pair* $(\mathbf{x}, \overline{\mathbf{x}})$ *which fulfills*

$$(M - \lambda D - \mu K) \cdot (\mathbf{x}, \overline{\mathbf{x}}) = \mathbf{o}, \quad \|\mathbf{x}\| = 1, \quad \mathbf{x} \cdot \overline{\mathbf{x}} = 0, \tag{4.8}$$

where D is as in Lemma 4.1.2, M is given by Equ. (4.4), K is from Equ. (2.28), and λ, μ satisfy

$$\det(M - \lambda D - \mu K) = 0. \tag{4.9}$$

Proof. With the matrices M, D, and K the minimization problem $F(\mathbf{x}, \overline{\mathbf{x}}) \to \min$, $\mathbf{x}^2 = 1$, $\mathbf{x} \cdot \overline{\mathbf{x}} = 0$ is transformed into to $F(\mathbf{x}, \overline{\mathbf{x}}) = (\mathbf{x}, \overline{\mathbf{x}})^T \cdot M \cdot (\mathbf{x}, \overline{\mathbf{x}}) \to \min$, $G(\mathbf{x}, \overline{\mathbf{x}}) = (\mathbf{x}, \overline{\mathbf{x}})^T \cdot D \cdot (\mathbf{x}, \overline{\mathbf{x}}) = 1$, $H(\mathbf{x}, \overline{\mathbf{x}}) = (\mathbf{x}, \overline{\mathbf{x}})^T \cdot K \cdot (\mathbf{x}, \overline{\mathbf{x}}) = 0$.

We introduce two Lagrangian multipliers λ, μ and solve $(\operatorname{grad}_F - \lambda \operatorname{grad}_G - \mu \operatorname{grad}_H)(\mathbf{x}, \overline{\mathbf{x}}) = 0$, $G(\mathbf{x}, \overline{\mathbf{x}}) = 1$, $H(\mathbf{x}, \overline{\mathbf{x}}) = 0$. This simplifies to Equ. (4.8). The nonzero vector $(\mathbf{x}, \overline{\mathbf{x}})$ is contained in the kernel of $M - \lambda D - \mu K$, which implies Equ. (4.9). Equ. (4.8) immediately shows that $F(\mathbf{x}, \overline{\mathbf{x}}) = \lambda$. □

The solution of this problem is not as straightforward as that of the previous one. Equ. (4.9) defines an algebraic curve in the (λ, μ)-plane. The set of solutions of (4.9) together with the equations $(M - \lambda D - \mu K) \cdot (\mathbf{x}, \overline{\mathbf{x}}) = \mathbf{o}$, $\|\mathbf{x}\| = 1$ in the variables $\lambda, \mu, \mathbf{x}, \overline{\mathbf{x}}$ is an algebraic variety in $\mathbb{R}^8$. Its projection onto the coordinate space $\mathbb{R}^6$ of variables $\mathbf{x}, \overline{\mathbf{x}}$ is, in the generic case, an algebraic curve Φ, because then for all pairs (λ, μ) satisfying (4.9) there are exactly two solutions of the other two equations.

The solutions of the minimization problem are contained in the intersections of the curve Φ with the Klein quadric, which corresponds to the equation $\mathbf{x} \cdot \overline{\mathbf{x}} = 0$.

Because of the high degree of the problem, we do not pursue further its algebraic aspects. The solution is best computed numerically. A good starting point for an iterative algorithm would be the approximant complex computed by minimizing (4.3).

Complexes of Infinite Pitch

Linear complexes $\mathcal{C}$ of infinite pitch consist of lines which intersect a certain line at infinity. In Euclidean space, the proper lines of such a complex comprise the set of lines orthogonal to a certain vector $\overline{\mathbf{c}}$. A line L with Plücker coordinates $(\mathbf{l}, \overline{\mathbf{l}})$ is in $\mathcal{C}$ if and only if $\mathbf{l} \cdot \overline{\mathbf{c}} = 0$.

Such complexes have been excluded from the discussion so far, because we worked with moments and they are defined only for complexes of finite pitch.

We define the deviation of a line L of Euclidean $\mathbb{R}^3$ from $\mathcal{C}$ by $|\cos \sphericalangle(L, \overline{\mathbf{c}})|$. The deviation of a complex $\mathcal{X}$ with Plücker coordinates $(\mathbf{o}, \overline{\mathbf{x}})$ with $\|\overline{\mathbf{x}}\| = 1$ from a given finite set $L_1, \ldots, L_k$ of lines with normalized Plücker coordinates $(\mathbf{l}_i, \overline{\mathbf{l}}_i)$ is defined by

$$F_\infty(\overline{\mathbf{x}}) = \sum_{i=1}^{k} (\overline{\mathbf{x}} \cdot \mathbf{l}_i)^2. \tag{4.10}$$

The minimization of $F_\infty(\overline{\mathbf{x}})$ subject to the side condition $\overline{\mathbf{x}}^2 = 1$ leads to an ordinary eigenvalue problem in $\mathbb{R}^3$.

Note that one might not know in advance whether an approximation of the given data with such a special case of a singular complex makes sense. Input data which

are actually contained in a complex of infinite pitch cause all coefficients in (4.7) to vanish (the vector $(0, \bar{\mathbf{c}})$ obviously is contained in the kernel of both M and D). Thus data which can be well approximated by such a complex can be detected by the magnitude of these coefficients.

Remark 4.1.3. If small coefficients in Equ. (4.7) cause numerical difficulties then of course one remedy is to approximate with a complex of infinite pitch. Another possibility is to use the normalization $\mathbf{x}^2 + \bar{\mathbf{x}}^2 = 1$ instead of $\mathbf{x}^2 = 1$. This is equivalent to letting $D = E_6$ and leads to an equation of degree six instead of the cubic equation (4.7). ◇

Pencils of Minimizing Complexes

It is possible that Equ. (4.7) of Lemma 4.1.2 has two small solutions λ_1, λ_2. This means that there are two solution complexes $\mathcal{C}_1$, $\mathcal{C}_2$ of Equ. (4.6) corresponding to λ_1 and λ_2, respectively, which fit the input data equally well. In fact, all complexes of the pencil spanned by $\mathcal{C}_1$, $\mathcal{C}_2$ are close to the input lines:

Lemma 4.1.4. *If $\mathcal{C}$ is a complex of the pencil spanned by $\mathcal{C}_1$, $\mathcal{C}_2$ with Plücker coordinates $\mathcal{C}_i\gamma^\star = (\mathbf{c}_i, \bar{\mathbf{c}}_i)\mathbb{R}$ $(i = 1, 2)$ and $\alpha = \sphericalangle(\mathbf{c}_1, \mathbf{c}_2)$, then for all lines L*

$$m(L, \mathcal{C}) \leq 1/|\sin\alpha| \cdot (m(L, \mathcal{C}_1) + m(L, \mathcal{C}_2)). \tag{4.11}$$

Proof. Assume that $L\gamma = (\mathbf{l}, \bar{\mathbf{l}})\mathbb{R}$ with $\|\mathbf{l}\| = 1$, that $\|\mathbf{c}_i\| = 1$ and that $\mathcal{C}\gamma = (\mathbf{c}, \bar{\mathbf{c}})\mathbb{R}$, $\|\mathbf{c}\| = 1$ with $(\mathbf{c}, \bar{\mathbf{c}}) = \mu_1(\mathbf{c}_1, \bar{\mathbf{c}}_1) + \mu_2(\mathbf{c}_2, \bar{\mathbf{c}}_2)$. Then $\mu_1, \mu_2 \leq 1/|\sin\alpha|$ and we have $m(L, \mathcal{C}) = |\mu_1(\mathbf{c}_1 \cdot \bar{\mathbf{l}} + \bar{\mathbf{c}}_1 \cdot \mathbf{l}) + \mu_2(\mathbf{c}_2 \cdot \bar{\mathbf{l}} + \bar{\mathbf{c}}_2 \cdot \mathbf{l})| \leq |\mu_1| \cdot m(L, \mathcal{C}_1) + |\mu_2| \cdot m(L, \mathcal{C}_2)$, so the lemma is proved. □

Lemma 4.1.4 shows that the input data in the case of two small solutions λ_1, λ_2 of (4.7) are close to all complexes of a pencil of complexes. In the generic case the carrier of this pencil (cf. Sec. 3.2) is a linear line congruence. We could also ask whether a line which is close to all complexes of a pencil G is also close to the lines of the carrier $C(G)$. The answer is affirmative, but we will not give precise estimates.

Remark 4.1.4. Assume that a pencil G of linear complexes is spanned by $\mathcal{C}_1$ and $\mathcal{C}_2$. Consider the set of lines L with $m(L, \mathcal{C}) < \varepsilon$ for all complexes $\mathcal{C} \in G$. The Klein image of this set of lines is bounded by a certain non-Euclidean distance surface. ◇

Bundles of Minimizing Complexes

It is possible that Equ. (4.7) has three small solutions λ_1, λ_2, λ_3. This means that there are three projectively independent solution complexes $\mathcal{C}_i$ of Equ. (4.6), which fit the input data equally well, and all complexes of the *bundle* G spanned by $\mathcal{C}_1, \mathcal{C}_2, \mathcal{C}_3$ are close to the input data. This is shown by applying Lemma 4.1.4 twice: We have an inequality of the form

$$m(L,\mathcal{C}) \le k \cdot \sum m(L,\mathcal{C}_i)$$

if $\mathcal{C}$ is a complex of G, with a constant k depending on the angles between the vectors $\mathbf{c}_i$, where $\mathcal{C}_i\gamma^\star = (\mathbf{c}_i, \bar{\mathbf{c}}_i)\mathbb{R}$.

Again it is possible to show that the lines close to *all* complexes of a bundle G are close to lines of the carrier $C(G)$, which is a regulus in the generic case. Approximation by reguli is discussed later (see p. 217). We first describe two degenerate cases.

Fitting Bundles to Lines

To fit lines L_i with a proper *line bundle*, i.e., one with a proper vertex, we choose two orthogonal planes $\sigma_i : \mathbf{m}_i \cdot \mathbf{x} - f_i = 0$ and $\tau_i : \mathbf{n}_i \cdot \mathbf{x} - g_i = 0$ which contain L_i. Without loss of generality we choose $\mathbf{m}_i$ and $\mathbf{n}_i$ as orthogonal unit vectors. The distance of a point $\mathbf{x}$ to the planes σ_i and τ_i equals $\mathbf{m}_i \cdot \mathbf{x} - f_i$ and $\mathbf{m}_i \cdot \mathbf{c} - g_i$, respectively, so the distance of $\mathbf{x}$ to the line L_i is computed by

$$d(\mathbf{x}, L_i)^2 = (\mathbf{m}_i \cdot \mathbf{x} - f_i)^2 + (\mathbf{n}_i \cdot \mathbf{x} - g_i)^2.$$

The vertex $\mathbf{v}$ of the approximating bundle is therefore found as minimizer of

$$\sum_{i=1}^{k} d(\mathbf{x}, L_i)^2 = \sum_{i=1}^{k} [(\mathbf{m}_i \cdot \mathbf{x} - f_i)^2 + (\mathbf{n}_i \cdot \mathbf{x} - g_i)^2]. \tag{4.12}$$

A bundle of parallel lines is fitted to the lines $L_1, \ldots, L_k$ in the following way: We may assume that there is a vector $\mathbf{w}_0$ and vectors $\mathbf{l}_i$ parallel to L_i such that $\mathbf{w}_0 \cdot \mathbf{l}_i > 0$ for all i. Then let

$$\mathbf{w} = \frac{1}{k} \sum \mathbf{l}_i.$$

The bundle of lines parallel to $\mathbf{w}$ then is the bundle which minimizes the sum of squared Euclidean distances (in $\mathbb{R}^3$) of $\mathbf{l}_i$ to $\mathbf{w}$.

Fitting Fields to Lines

This problem is dual to the previous one, so we could solve it by applying some duality to the input data, fitting a bundle to it, and applying the inverse duality to this bundle. But this has the disadvantage that the resulting field is no longer minimizing any distances defined by Euclidean geometry.

On the other hand imagine a plane ε and a line L nearly parallel to it. There is a line segment in L whose points are all close to ε, but the distances of L's points to ε may become arbitrarily large. That is why it is better to solve a different problem: The fitting of a field to *line segments*, which is discussed below.

Fitting Complexes to Line Segments

In applications it often makes sense to define the deviation of a line L from some unbounded set M by intersecting this line with a certain domain of interest D and considering the deviation of $L \cap D$ from M. A simple special case is to choose a segment in L. We will show how to modify the algorithms for fitting linear complexes to lines such that they become algorithms for fitting linear complexes to line segments.

We need an appropriate definition of the distance of a line segment $\overline{\mathbf{ab}}$ to a linear complex $\mathcal{C}$ with equation $\bar{\mathbf{c}} \cdot \mathbf{l} + \mathbf{c} \cdot \bar{\mathbf{l}} = 0$ and corresponding null polarity π: By Equ. (3.3), the lines of $\mathcal{C}$ incident with $\mathbf{a}$ are contained in the plane $\mathbf{a}\pi$ with normal vector $\mathbf{n}_\mathbf{a} = \bar{\mathbf{c}} + \mathbf{c} \times \mathbf{a}$. The distance of $\mathbf{b}$ to this plane is given by

$$d(\mathbf{b}, \mathbf{a}\pi) = \frac{|\mathbf{n}_\mathbf{a} \cdot (\mathbf{b} - \mathbf{a})|}{\|\mathbf{n}_\mathbf{a}\|}.$$

Assume that the line $L = \mathbf{a} \vee \mathbf{b}$ has Plücker coordinates $(\mathbf{l}, \bar{\mathbf{l}})$ with $\mathbf{l} = \mathbf{b} - \mathbf{a}$. Then by insertion of $\mathbf{n}_\mathbf{a}$

$$d(\mathbf{b}, \mathbf{a}\pi) = \frac{\bar{\mathbf{c}} \cdot \mathbf{l} + \mathbf{c} \cdot \bar{\mathbf{l}}}{\|\bar{\mathbf{c}} + \mathbf{c} \times \mathbf{a}\|}. \tag{4.13}$$

Obviously interchanging $\mathbf{a}$ and $\mathbf{b}$ gives an analogous expression for the distance $d(\mathbf{a}, \mathbf{b}\pi)$. This motivates the following

Definition. *With the notation of the previous paragraph, the distance $d(\overline{\mathbf{ab}}, \mathcal{C})$ between the line segment $\overline{\mathbf{ab}}$ and the complex $\mathcal{C}$ is defined by*

$$d(\overline{\mathbf{ab}}, \mathcal{C})^2 = d(\mathbf{b}, \mathbf{a}\pi)^2 + d(\mathbf{a}, \mathbf{b}\pi)^2 = (\bar{\mathbf{c}} \cdot \mathbf{l} + \mathbf{c} \cdot \bar{\mathbf{l}})^2 \left(\frac{1}{v_\mathbf{a}^2} + \frac{1}{v_\mathbf{b}^2} \right),$$
$$\textit{where} \quad \mathbf{l} = \mathbf{b} - \mathbf{a}, \quad v_\mathbf{a} = \|\bar{\mathbf{c}} + \mathbf{c} \times \mathbf{a}\|, \quad v_\mathbf{b} = \|\bar{\mathbf{c}} + \mathbf{c} \times \mathbf{b}\|. \tag{4.14}$$

If the line spanned by the points $\mathbf{a}$ and $\mathbf{b}$ is contained in $\mathcal{C}$, then $d(\overline{\mathbf{ab}}, \mathcal{C}) = 0$.

Remark 4.1.5. The complex $\mathcal{C}$ defines a uniform helical motion (cf. Th. 3.1.6). Then $v_\mathbf{a}$ is the norm of the velocity vector $\mathbf{n}_\mathbf{a}$ of the point $\mathbf{a}$. If p is the pitch of $\mathcal{C}$ and and $r_\mathbf{a}$ is the distance of $\mathbf{a}$ from $\mathcal{C}$'s axis, then

$$v_\mathbf{a} = \sqrt{r_\mathbf{a}^2 + p^2}. \qquad \diamond$$

The linear complex $\mathcal{X}$ which fits the line segments $\overline{\mathbf{a}_1\mathbf{b}_1}, \ldots, \overline{\mathbf{a}_k\mathbf{b}_k}$ best is defined to be the minimizer of

$$\sum_{i=1}^{k} d(\overline{\mathbf{a}_i\mathbf{b}_i}, \mathcal{X})^2 = \sum_{i=1}^{k} \left(\frac{1}{v_{\mathbf{a}_i}^2} + \frac{1}{v_{\mathbf{b}_i}^2} \right) (\bar{\mathbf{x}} \cdot \mathbf{l}_i + \mathbf{x} \cdot \bar{\mathbf{l}}_i)^2, \tag{4.15}$$

where $\mathbf{l}_i = \mathbf{b}_i - \mathbf{a}_i$, $\bar{\mathbf{l}}_i = \mathbf{a}_i \times \mathbf{l}_i = \mathbf{b}_i \times \mathbf{l}_i$, and $v_{\mathbf{a}_i}$, $v_{\mathbf{b}_i}$ are the velocities of $\mathbf{a}_i$, $\mathbf{b}_i$ as defined by Equ. (4.14). The solution may be computed using *weight iteration*: We minimize the weighted sum

$$F(\mathbf{x}, \overline{\mathbf{x}}, w_1, \ldots, w_k) = \sum_{i=1}^{k} w_i (\overline{\mathbf{x}} \cdot \mathbf{l}_i + \mathbf{x} \cdot \overline{\mathbf{l}}_i)^2, \tag{4.16}$$

subject to an appropriate side condition which expresses a normalization of $(\mathbf{x}, \overline{\mathbf{x}})$: Typically this would be $\|\mathbf{x}\| = 1$, but if a solution complex of very large pitch is expected it is better to use $\|\overline{\mathbf{x}}\| = 1$. The solution is analogous to the one described by Lemma 4.1.2. In the beginning we let $w_1 = \cdots = w_k = 1$. After the first step we use

$$w_i = 1/v_{\mathbf{a}_i}^2 + 1/v_{\mathbf{b}_i}^2, \quad i = 1, \ldots, k,$$

where $v_{\mathbf{a}_i}, v_{\mathbf{b}_i}$ are defined by Equ. (4.14), and compute a new minimizer of (4.16). This is iterated until the change of weights from step to step is less than some threshold value.

To complete the discussion of singular cases in the previous section, we mention how to fit a field of lines to given line segments $\overline{\mathbf{a}_i \mathbf{b}_i}$. The simplest solution of this problem is to find a plane approximating the points $\mathbf{a}_i$, $\mathbf{b}_i$ in the usual least-squares sense.

This procedure can be used to find a field of lines which fits given *lines* $L_1, \ldots, L_k$ within a bounded region of interest $D \subset E^3$. We simply use the smallest line segments $\overline{\mathbf{a}_i \mathbf{b}_i}$ which contain the intersection $L_i \cap D$.

4.2 Kinematic Surfaces

As an application of the theoretical problem of fitting linear complexes to given lines or line segments, we look at a problem which arises in the context of *reverse engineering* of geometric models [196]: Given are scattered data points which are expected to fit to a simple surface, where the meaning of 'simple' is explained later in this section. We want to reconstruct the surface or the geometric data which uniquely determine it.

A particular instance of this problem is the automated reconstruction of parts from laser scanner data and the decomposition of their boundary surface in its planar, cylindrical, etc., pieces [118, 155, 158, 195].

This section is organized as follows: First we determine surfaces which are invariant with respect to uniform motions and show that their surface normals are contained in certain linear manifolds of lines. The next topic is the estimation of these linear manifolds from scattered surface normals, and how to compute the surfaces from them. Last we discuss the reconstruction of surfaces which are 'piecewise almost' invariant.

Consider a one-parameter subgroup $M(t)$ of Euclidean motions (a uniform helical, rotational or translational motion, cf. Th. 3.4.3) and a curve $c : I \to E^3$ in Euclidean three-space. The symbol

$$g(u, v) = M(u)(c(v)), \quad u \in \mathbb{R},\ v \in I. \tag{4.17}$$

means that we apply the Euclidean motion $M(u)$ to the curve point $c(v)$. Then g parametrizes a surface in Euclidean space. It is a *cylindrical surface* or *cylinder* if $M(t)$ is a group of translations, a *surface of revolution*, if $M(t)$ is a group of rotations about an axis, and a *helical surface* otherwise. We refer to these types of surface as *kinematic surface*.

Remark 4.2.1. A subset of Euclidean space may be a kinematic surface in several ways: The cylinder of revolution is an example of a surface which is at the same time a cylindrical surface, a surface of revolution, and a helical surface (see Fig. 4.1, right). ◇

Invariant Surfaces

Clearly the surfaces described by Equ. (4.17) are *invariant* with respect to the one-parameter group of motions which generates them: If p is a point of the surface, then so is $M(t)(p)$ for all $t \in \mathbb{R}$ (see Fig. 4.1). We ask for all surfaces which are invariant under the one-parameter group $M(t)$:

Theorem 4.2.1. *A subset Φ of Euclidean space E^3 which is both a two-dimensional C^1 submanifold and invariant with respect to a one-parameter group of motions $M(t)$ is a kinematic surface as described by Equ. (4.17).*

Proof. (Sketch) It is sufficient to prove this locally. Choose a point $p \in \Phi$ whose velocity vector $v_p = d/dt|_{t=0} M(t)(p)$ is nonzero and consider a curve $c : I \to E^3$ with $c(0) = p$ and with $\{\dot{c}(0), v_p\}$ linearly independent, such that the surface $g(u, v) = M(u)(c(v))$ is locally regular. The point $g(u, v)$ is contained in Φ by invariance of Φ. Thus g locally is a diffeomorphism of an open neighbourhood of $(0, 0)$ in the u, v parameter domain to an open subset of Φ, and Φ is locally parametrized as a kinematic surface.

If $v_p = 0$, there is nothing to show, because $M(t)(p) = p$ for all t. □

There is a simple characterization of invariant surfaces, respectively, kinematic surfaces, in terms of their normals:

Lemma 4.2.2. *The surface normals of a regular C^1 surface $g : U \subset \mathbb{R}^2 \to E^3$ are contained in a linear complex if and only if the surface is contained in a kinematic surface as defined by Equ. (4.17).*

Proof. The surface normals of a kinematic surface are path normals of the curves $M(t)(p)$, and so the 'if' part of the theorem follows from Th. 3.1.6.

To prove the converse, assume that all of g's surface normals are contained in a linear complex $\mathcal{C}$, which, by Th. 3.1.6, is the path normal complex of a one-parameter group $M(t)$ of motions. We consider a point $p = g(u_0, v_0)$ (cf. Fig. 4.1, left). The image $g(V)$ of a small neighbourhood V of (u_0, v_0) is a two-dimensional C^1 submanifold of E^3. The integral curves of M's velocity vector field $v : p \mapsto v(p)$ are tangent to $g(U)$ by our assumption, which shows that especially the integral

curve $M(t)(p)$ starting in p is contained in $g(V)$. Fig. 4.1, left, shows a sequence of such integral curves, which are helices.

Now we can choose a curve $c : I \to g(V)$ such that $c(0) = p$ and $\{\dot{c}(0), v(p)\}$ is linearly independent. The kinematic surface $h(t, s) = M(t)(c(s))$ locally parametrizes $g(V)$, and the proof is complete. □

Fig. 4.1, left shows a helical surface generated as envelope of a sphere which undergoes a uniform helical motion. This surface is both an invariant surface and a pipe surface, which means envelope of a smooth family of spheres.

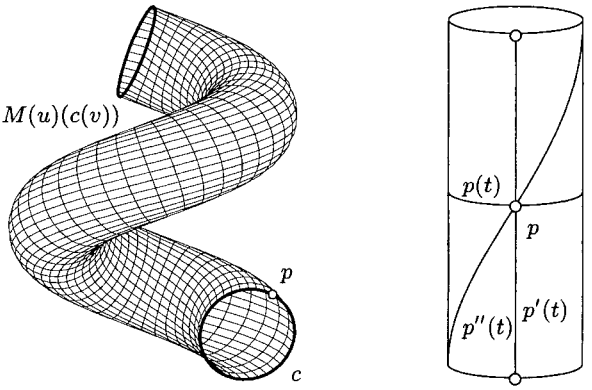

Fig. 4.1. Left: Helical pipe surface. Right: A cylinder is a multiply invariant surface: point p with paths $p(t), p'(t), p''(t)$ corresponding to different one-parameter groups of motions leaving the surface invariant.

Multiply Invariant Surfaces

It is important to know which surfaces are invariant with respect to more than just one one-parameter group. Before answering that question, we prove the following

Lemma 4.2.3. *If C_1, C_2 are two different linear complexes, and $M_1(t)$, $M_2(t)$ are corresponding one-parameter groups of motions, and a linear line congruence is invariant with respect to both $M_1(t)$, $M_2(t)$, then this congruence is a bundle of lines, or a field of lines, or consists of all lines which intersect a proper line orthogonally.*

Proof. Clearly the possibilities mentioned have this property. The converse is also shown easily: A hyperbolic congruence is invariant only if both its axes are invariant, but non-intersecting and non-parallel lines invariant under rotations and helical motions are only the axis and the ideal line orthogonal to it.

A parabolic congruence is not invariant with respect to any Euclidean motion, which follows from from the detailed description in Sec. 3.2.2.

An elliptic linear congruence can have rotational symmetry, like the one described by Equ. (3.15). It is left to the reader as an exercise to show that no elliptic congruence can be multiply invariant (this follows from Prop. 3.2.8). □

The following lemma enumerates all surfaces which are multiply invariant. The result is intuitively clear anyway (cf. Fig. 4.1, right).

Lemma 4.2.4. *A connected regular C^1 surface $g : U \to E^3$, all of whose surface normals are contained in two different linear complexes $\mathcal{C}_1$, $\mathcal{C}_2$, is contained in a plane, or sphere, or cylinder of revolution.*

Proof. Denote the pencil of linear complexes spanned by $\mathcal{C}_1$ and $\mathcal{C}_2$ by G. If N is a surface normal, then by Lemma 3.2.2, $N \in \mathcal{C}_1$, $N \in \mathcal{C}_2$ is equivalent to $N \in C(G)$.

If $\mathcal{C} \in G$ and $M(t)$ is the uniform motion whose path normal complex equals $\mathcal{C}$, then Lemma 4.2.2 shows that the surface $g(U)$ locally is a kinematic surface with respect to $M(t)$. As $C(G)\gamma$ is a two-dimensional quadric, it is determined by the surface normals of arbitrarily small open subsets of $g(U)$. This implies that $C(G)$ is invariant by such an $M(t)$, and so $C(G)$ must be as described by Lemma 4.2.3.

We now choose special uniform motions $M(t)$, namely: (i) if $C(G)$ is degenerate with a proper vertex O, consider all rotations about O; if (ii) $C(G)$ is degenerate with an ideal vertex A_u, choose all translations orthogonal to A_u; if (iii) $C(G)$ is hyperbolic with proper axis A, choose a rotation about A and a translation parallel to A. The last remaining case, a field of lines, cannot occur. The statement we want to prove now follows locally from Lemma 4.2.2 and globally from connectedness of $g(U)$. Cases (i), (ii), and (iii) correspond to the sphere, the plane, and the cylinder of revolution. □

Corollary 4.2.5. *The only connected surfaces which are invariant with respect to two independent one-parameter groups of Euclidean motions are spheres, planes, and cylinders of revolution.*

Fitting Complexes to Scattered Surface Normals

To approximate scattered data points $p_1, \ldots, p_k$ by a kinematic surface we proceed as follows: First we estimate the surface normals $N_1, \ldots, N_k$ at the data points. There exist solutions of this problem which will not be discussed here (see e.g. [78]). We assume that the input data are evenly distributed. If not, we have to apply data reduction algorithms first (see [122]). Lemma 4.2.2 shows that in order to find the one-parameter subgroup which generates the approximating kinematic surface, we have to fit a linear complex $\mathcal{C}$ to the surface normals. This is done by using the methods described in this section. With Equ. (3.9) we compute axis A and pitch p of the generating motion. Of course there are several different cases according to dimensionality of the solution and magnitude of the pitch.

1. If p is small compared to the diameter of the input point cloud we may want to fit a complex of zero pitch to the input normals. This corresponds to input data with rotational symmetry.

2. If p is very large, we could fit a linear complex of infinite pitch. This leads to a cylindrical surface which approximates the input data.
3. If a pencil of complexes fits the input normals, Cor. 4.2.5 shows that they are close to the surface normals of spheres, planes, or cylinders.

Remark 4.2.2. Small portions of input data will often lead to a pencil of nearly equally good solutions and it depends on further information what one can do in this case: If the input data are not expected to be multiply invariant, we may be able to gather more sample points and run the approximation algorithm again. If a kinematic surface fits the input data well in small regions, we have to paste together pieces of kinematic surfaces. This is discussed below. ◇

Remark 4.2.3. In reverse engineering applications the input data can have large measurement errors or possibly include data points which belong to another part of the object which does not fit the same kinematic surface.

Thus an approximation method must be able to cope with outliers, which is not the case for the least squares method in the form presented above. Therefore, one may use a robust regression method to compute an initial estimate (e.g., an estimate of a least median of squares solution) and then refine it by either rejecting outliers or by down-weighting their influence on the final approximant.

This kind of noise filtering based on so-called *M-estimators* has been investigated in detail both in statistics and in computer vision. Note that the formulae presented here are nicely compatible with M-estimation, since we just have to reformulate the various functions F to be minimized as a weighted sum of squares of moments, using one of the weighting schemes suggested in the literature [171]. ◇

Remark 4.2.4. The minimization of the function F of Equ. (4.3) is motivated by the following approach: Consider the one-parameter group $M(t)$ of helical motions associated with a linear complex $\mathcal{C}$ with $\mathcal{C}\gamma^\star = (\mathbf{c}, \overline{\mathbf{c}})\mathbb{R}$, $\|\mathbf{c}\| = 1$. The velocity $\mathbf{v}(\mathbf{x})$ of the point $\mathbf{x}$ is given by Equ. (3.25). Assume that we have found estimates N_i of surface normals at the data points $\mathbf{x}_i$, which have normalized Plücker coordinates $(\mathbf{n}_i, \overline{\mathbf{n}}_i)$. Then

$$\cos\gamma_i = \cos\sphericalangle(\mathbf{v}(\mathbf{x}_i), \mathbf{n}_i) = \frac{\mathbf{n}_i \cdot \mathbf{v}(\mathbf{x}_i)}{\|\mathbf{v}(\mathbf{x}_i)\|} = \frac{\overline{\mathbf{c}} \cdot \mathbf{n}_i + \mathbf{c} \cdot \overline{\mathbf{n}}_i}{\|\mathbf{v}(\mathbf{x}_i)\|}.$$

Minimizing the function

$$G(\mathbf{c}, \overline{\mathbf{c}}) = \sum_{i=1}^{k} \cos^2\gamma_i$$

with the side condition $\|\mathbf{c}\| = 1$ is a nonlinear problem. We did minimize the function F of Equ. (4.3). Equ. (4.2) shows that

$$F(\mathbf{c}, \overline{\mathbf{c}}) = \sum_{i=1}^{k} (r_i^2 + p^2) \cos^2\gamma_i,$$

where r_i is the distance of data point $\mathbf{d}_i$ to the axis of $\mathcal{C}$. This is a reasonable and geometrically meaningful simplification of $G \to \min$. In fact by using a weight iteration as in Equ. (4.16) it is even possible to minimize G. ◇

Fitting Kinematic Surfaces to Scattered Data Points

After we have found a one-parameter subgroup $M(t)$ of Euclidean motions which fits the estimates of surface normals, we try to find the approximating surface itself. This is done by 'projecting' the input data points $\mathbf{d}_i$, $i = 1, \ldots, k$ into an appropriate plane ε, where the image of the point $\mathbf{d}_i$ is found by following its trajectory $M(t)(\mathbf{d}_i)$ until it intersects ε. As the trajectories of points may intersect planes more often than once (indeed, even infinitely many times), this definition has to be more precise in order to make the projection well defined:

1. If $M(t)$ is subgroup of translations, the only restriction is that ε must not be parallel to the trajectories of points. It makes sense to choose the plane orthogonal to the vector of the translation.
2. If $M(t)$ is a subgroup of rotations about a fixed axis A, we choose ε such that it contains A. Then all trajectories except those of A's points will intersect ε in two points (see Fig. 4.2).
   The mapping becomes well defined if we choose one of the two closed half-planes defined by A in ε and intersect all trajectories with this half-plane.
3. If $M(t)$ is a uniform helical motion of pitch p and axis A, choose ε orthogonal to A. Then all trajectories intersect ε once. It turns out that for actual computations this choice is not always the best, especially if p is small.
   A choice which works well in practice is to choose ε as the path normal plane of one of the data points. All trajectories intersect this plane in a finite number of points. If the points are close together the intersection points cluster in a finite number of well separated subsets.

After performing the intersection, the points $\mathbf{p}_i$ should lie close to a certain curve, if the original points lie close to a kinematic surface. This curve can be fitted to the points $\mathbf{p}_i$ (cf. [106, 158] and Fig. 4.2). The surface generated by this curve under the action of $M(t)$ is the approximant we have been looking for.

Remark 4.2.5. 'Projecting' data points into a reference plane should keep artificial distortions to a minimum. In cases 1 and 2 of the above list, the distance of a data point to the eventual solution surface is the same as the distance of the projected point to the curve which is fitted to these projected points.

In case 3, however, the first method, which always works, does not have this property — the smaller p and the farther the data points are from the axis, the more distances increase. The second method of projection is less trivial in its implementation, but avoids these distortions to a certain extent. ◇

Fitting Special Surfaces

In computer-aided design, simple surfaces whose normals form a well known subset of line space occur very often. These include planes, spheres, cylinders or cones of revolution, and tori, some of which are multiply invariant. It is useful to specialize the general approximation algorithms for these surfaces:

1. A plane is easily fitted to scattered data points, so if the input data are known to be contained in a plane, the whole machinery described above is actually not necessary.
2. A line is easily fitted to scattered data points in a plane. This situation occurs when the original data points belong to a part of a half-cone of revolution, where half-cone means one of the two halves of a cone which are separated by the vertex. After reconstruction of the axis A and projecting the input data into a half-plane as described above, a line has to be fitted to the projections of points.
3. A sphere with center $\mathbf{x}$ is fitted to scattered points $\mathbf{p}_i$ by minimizing

$$F(\mathbf{x}) = \sum_{i,j} \frac{((2\mathbf{x} - \mathbf{p}_i - \mathbf{p}_j) \cdot (\mathbf{p}_i - \mathbf{p}_j))^2}{\|\mathbf{p}_i - \mathbf{p}_j\|^2}, \tag{4.18}$$

   where summation is over all index pairs i, j such that $\|\mathbf{p}_i - \mathbf{p}_j\|$ is not too small compared with the extension of the point cloud $\mathbf{p}_i$.
   The motivation for this is the following: The single terms in this sum are the squared distances of the point $\mathbf{x}$ to the bisector plane of $\mathbf{p}_i$ and $\mathbf{p}_j$, which is numerically ill-defined if $\|\mathbf{p}_i - \mathbf{p}_j\|$ is small.
4. A circle is fitted to points in a plane by minimizing the same expression, with the only difference that the variables (4.18) are vectors of $\mathbb{R}^2$. This occurs if the input data belong to a torus: After projection of the data points to a half-plane which contains the axis we have to fit a circle to these points.

For solutions of the problem of fitting special surfaces based on their representation as algebraic varieties, we refer to the literature [118, 163].

Example 4.2.1. This example concerns scattered data (e.g. obtained by a laser scanner) from an object whose boundary is a surface of revolution. The surface normals at the data points are estimated (see Fig. 4.2, left). The pitch in this case is nearly zero, which shows that the original data come from a surface of revolution. We let $p = 0$ and project the input data into a half-plane which contains the axis (Fig. 4.2, center). The curve which fits these points was found by a moving least squares method according to [106]. ◇

Example 4.2.2. We again consider reconstruction of surfaces from scattered data. The difference to Ex. 4.2.1 is that the data do not come from a surface of revolution, but from a *pipe surface*, which is defined as the envelope of spheres of equal radius whose center runs in the *spine curve*.

A pipe surface is locally well approximated by a surface of revolution: If we replace the spine curve by its osculating circle, we get a torus which is in second

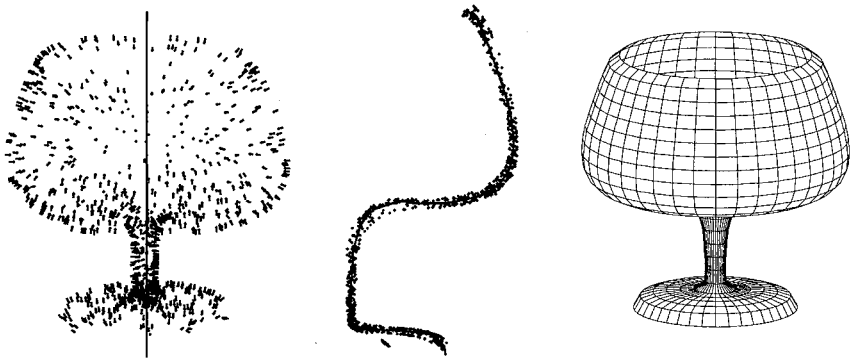

Fig. 4.2. Reconstruction of a surface of revolution: Left: data points, estimates of normal vectors, and axis computed from this estimation. Center: points projected onto a plane and a curve approximating this point set, Right: final surface of revolution.

order contact with the pipe surface in all points of a common circle. If we consider only small parts of the given point cloud, it is easy to determine such approximating tori, whose spine curves then locally approximate the spine curve of the pipe surface. The result of such an approximation is shown in Fig. 4.3. An application of this is the recovery of constant radius rolling ball blends in reverse engineering [99]. Using locally approximating surfaces of revolution, we can also reconstruct so-called moulding surfaces [108]. These are generated by a moving planar curve, whose carrier plane rolls on a cylinder surface. With local fits by right circular cones or cylinders, the reconstruction of developable surfaces may be performed [25]. ◇

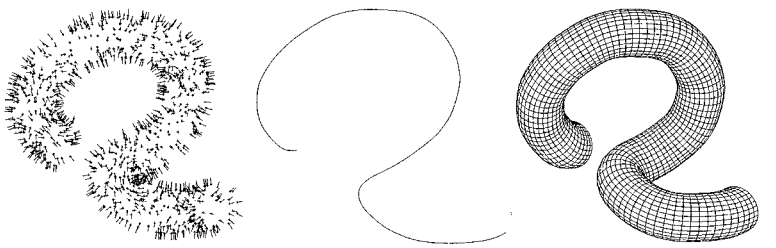

Fig. 4.3. Pipe surface: Left: data points and estimates of normal vectors, Center: approximate spine curve, Right: reconstruction of pipe surface.

Example 4.2.3. Fig. C.3 illustrates reverse engineering of an actual object.

This object is one of the so-called Darmstadt benchmarks suggested by J. Hoschek; the pictures were generated by the BSolid prototype Reverse Engineering

system, developed by the Computer and Automation Research Institute and Cadmus Consulting and Development Ltd., Budapest. ◇

Approximation by Kinematic Surfaces Using Additional Information

Reverse engineering of CAD models might also make use of further geometric information such as parallelity, concentricity, or orthogonality, if available.

1. If the direction $\mathbf{x}$ of the axis A of a surface of revolution is known in advance, minimization of the function $F(\mathbf{x}, \bar{\mathbf{x}})$ of Equ. (4.3) is much easier, because the constraint $\|\mathbf{x}\| = 1$ can be fulfilled automatically, and $\mathbf{x} \cdot \bar{\mathbf{x}} = 0$ is now a linear side-condition.
2. Similarly, the problem simplifies if we reconstruct a surface of revolution and know a point $\mathbf{b}$ of the axis A. If A's normalized Plücker coordinates are $(\mathbf{x}, \bar{\mathbf{x}})$, then $\bar{\mathbf{x}} = \mathbf{b} \times \mathbf{x}$ and $F(\mathbf{x}, \bar{\mathbf{x}})$ of Equ. (4.3) is a function of $\mathbf{x}$ alone. The constraint $\mathbf{x} \cdot \bar{\mathbf{x}} = 0$ is fulfilled automatically.
   Thus minimizing F is an ordinary eigenvalue problem.
3. An analogous situation occurs when fitting a surface of revolution, whose axis is constrained in a plane. Suppose that this plane is defined by a point $\mathbf{b}$ and two independent basis vectors $\mathbf{v}_1, \mathbf{v}_2$. We let $\mathbf{n} = \mathbf{v}_1 \times \mathbf{v}_2$ and have the linear relations

$$\mathbf{x} = \rho_1 \mathbf{v}_1 + \rho_2 \mathbf{v}_2, \quad \bar{\mathbf{x}} = (\mathbf{b} + \tau_1 \mathbf{v}_1 + \tau_2 \mathbf{v}_2) \times \mathbf{x} = \mathbf{b} \times \mathbf{x} + \tau \mathbf{n}.$$

   Thus the function F may be expressed in terms of ρ_1, ρ_2, τ.
4. Finally, if the axis has to intersect a given line L with Plücker coordinates $\mathbf{l}, \bar{\mathbf{l}}$, we have to make use of the linear intersection condition

$$\bar{\mathbf{x}} \cdot \mathbf{l} + \mathbf{x} \cdot \bar{\mathbf{l}} = 0.$$

   The minimization of F subject to this condition together with the normalization $\|\mathbf{x}\| = 1$ is similar to minimization of F subject to the condition that $\mathbf{x} \cdot \bar{\mathbf{x}} = 0$.

Remark 4.2.6. The first three cases in the list above lead to the minimization of a quadratic function subject to a normalization condition. This common property can also be seen in the Klein image: In line-geometric terms, we are looking for an approximant complex whose Klein image must lie in a certain projective subspace U of P^5:

For helical surface reconstruction without additional constraints (cf. Lemma 4.1.2), we can define $U = P^3$, which is actually no restriction. For reconstruction of surfaces of revolution in cases 1–3 of the above list, U is a plane contained in the Klein quadric:

In case 1, this plane is the Klein image of all lines parallel to a given vector. In case 2, this plane is the Klein image of all lines incident with the point $\mathbf{b}$. In case 3, this plane is the Klein image of a field. The fact that U is a subset of the Klein quadric explains why the quadratic side condition $\mathbf{x} \cdot \bar{\mathbf{x}} = 0$ is fulfilled automatically in cases 1–3.

Case 4 of the list above is different, as is the problem of finding a minimizing singular complex (cf. Lemma 4.1.3): Here the solution complexes are restricted to a quadratic variety V in P^5. In the case of singular complexes, V is the Klein quadric. In case 4 of the above list V is a tangential intersection of the Klein quadric. $\diamond$

4.3 Approximation via Local Mappings into Euclidean 4-Space

In this section we discuss approximation methods in line space which are based on local mappings into Euclidean 4-space. 'Local' means that these mappings are defined in open subsets of line space. It does not necessarily mean that these subsets are small.

Stereographic Projection

It is sometimes useful to identify a part of a quadric with an affine space. One familiar example is a map projection which identifies part of the globe with (part of) a sheet of paper.

Definition. *Assume that Φ is a quadric in P^n, the point Z is in Φ, and Q is a hyperplane with $Z \notin Q$. Then the projection*

$$\sigma : \Phi \to Q, \quad X \mapsto X\sigma = (X \vee Z) \cap Q \tag{4.19}$$

is called the stereographic projection of Φ to Q with center Z.

An example of a stereographic projection has been given in Ex. 1.1.37.

Lemma 4.3.1. *We use the notation of the definition above. If T is Φ's tangent plane at the center Z, then the stereographic projection is a one-to-one correspondence between $\Phi \setminus T$ and $Q \setminus T$. Hyperplanar sections Φ' of Φ are mapped onto $(n-2)$-dimensional projective subspaces of Q if and only if Φ' contains the projection center.*

Proof. We know that all lines not tangent to Φ intersect Φ in exactly two points or not at all. This shows that especially all non-tangential lines $Z \vee X$ with $X \in Q$ intersect the quadric Φ in exactly one further point besides Z. Thus $\sigma : \Phi \setminus T \to\to Q \setminus T$ is one-to-one and onto.

If $\Phi' = \Phi \cap H$, where H is a hyperplane, then Φ' contains Z if and only if H contains Z, so $Z \vee H$ is $(n-1)$-dimensional (otherwise, if Φ' does not contain Z, it has dimension n), and the statement follows. $\square$

The meaning of Lemma 4.3.1 is the following: If we disregard all points of Φ which are also contained in the center's tangent plane, the stereographic projection gives a one-to-one correspondence between the quadric and the *affine space* $Q \setminus T$.

Example 4.3.1. (cf. Ex. 1.1.37) We consider the projective extension of Euclidean space E^3. If Φ is the unit sphere, Z is its north pole, and Q is the equator plane, then besides Z there are no points of Φ which are contained in the north poles' tangent plane T. The line $T \cap Q$ is at infinity. Lemma 4.3.1 says that the stereographic projection is a one-to-one correspondence between the points of the unit sphere different from the north pole, and the points of the equator plane. ◇

Stereographic Projection of the Klein Quadric

The set $\mathcal{L}$ of the lines of three-dimensional projective space can be identified, via the Klein mapping, with the Klein quadric $M_2^4 \subset P^5$. The set $\mathcal{L}^o$ of proper lines of Euclidean space can be identified with the Klein quadric without a plane, which is the Klein image of the ideal field of lines (cf. Sec. 2.1.3). Unfortunately $\mathcal{L}^o$ (or its Klein image) does not have the structure of an affine space. Therefore we try to find an appropriate stereographic projection which identifies a certain subset of $\mathcal{L}$ with an affine space.

If L_Z is a line, then $Z := L_Z\gamma \in M_2^4$. The tangent plane of M_2^4 at Z contains the γ-images of all lines which intersect L_Z. We introduce a Cartesian coordinate system in E^3 and let Z equal the horizontal line at infinity, which is contained in all planes $z = \text{const}$. Then $L_Z\gamma = Z = (0,0,0,0,0,1)\mathbb{R}$.

A line L of Euclidean space, which does not intersect L_Z, i.e., is not horizontal, intersects both planes $\pi_- : z = 0$ and $\pi_+ : z = 1$ in points $\mathbf{x}_- = (x_1, x_2, 0)$ and $\mathbf{x}_+ = (x_3, x_4, 1)$. The Plücker coordinates of L are computed by

$$\begin{aligned} L\gamma &= (1, x_1, x_2, 0) \wedge (1, x_3, x_4, 1)\mathbb{R} \\ &= (x_3 - x_1, x_4 - x_2, 1, x_2, -x_1, x_1x_4 - x_2x_3)\mathbb{R}. \end{aligned} \tag{4.20}$$

P^5 is equipped with homogeneous coordinates $(x_{01} : \ldots : x_{12})$. The hyperplane $Q : x_{12} = 0$ does not contain the center Z, and projection of $L\gamma$ onto Q from the center Z gives the point

$$(Z \vee L\gamma) \cap Q = (x_3 - x_1, x_4 - x_2, 1, x_2, -x_1, 0)\mathbb{R}.$$

Thus x_1, x_2, x_3, x_4 are affine coordinates in the hyperplane Q, and the mapping

$$\sigma : L \in \mathcal{L}^o \mapsto (x_1, x_2, x_3, x_4) \in \mathbb{R}^4 \tag{4.21}$$

is, apart from a linear coordinate transformation, nothing but the stereographic projection.

Distances between Lines

We have to define a distance function between lines. If we restrict ourselves to non-horizontal lines L, we can use the stereographic projection σ defined by Equ. (4.21): If q is a positive definite quadratic form in $\mathbb{R}^4$, then $\sqrt{q(G\sigma - H\sigma)}$ serves as a *distance* between lines G, H.

We give a more detailed construction of such a distance function: We use the intersection points of lines with the planes $\pi_- : z = 0$ and $\pi_+ : z = 1$. If G, H are two non-horizontal lines, denote the four intersection points by $\mathbf{g}_- = (g_1, g_2, 0)$, $\mathbf{g}_+ = (g_3, g_4, 1)$, $\mathbf{h}_- = (h_1, h_2, 0)$, $\mathbf{h}_+ = (h_3, h_4, 1)$. With the notation of Equ. (4.21), $G\sigma = (g_1, g_2, g_3, g_4)$, $H\sigma = (h_1, h_2, h_3, h_4)$.

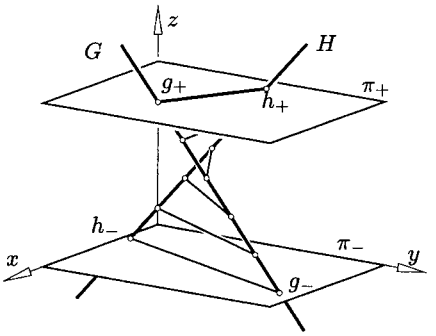

Fig. 4.4. Distance between lines measured horizontally.

We consider the correspondence

$$(1-\lambda)\mathbf{g}_- + \lambda\mathbf{g}_+ \mapsto (1-\lambda)\mathbf{h}_- + \lambda\mathbf{h}_+, \ \lambda \in [0,1],$$

(cf. Fig. 4.4) between the line segments $[\mathbf{g}_-, \mathbf{g}_+]$ and $[\mathbf{h}_-, \mathbf{h}_+]$. The lines which connect associated points are all horizontal and are contained in a hyperbolic paraboloid (by Prop. 1.1.40), or in a plane (if G, H are coplanar). An average distance of associated points is then given by

$$\begin{aligned} d(G,H)^2 &= 3\int_0^1 [(1-\lambda)(\mathbf{g}_- - \mathbf{h}_-) + \lambda(\mathbf{g}_+ - \mathbf{h}_+)]^2 d\lambda \qquad (4.22) \\ &= (\mathbf{g}_- - \mathbf{h}_-)^2 + (\mathbf{g}_+ - \mathbf{h}_+)^2 + (\mathbf{g}_- - \mathbf{h}_-)\cdot(\mathbf{g}_+ - \mathbf{h}_+). \end{aligned}$$

Because of

$$d(G,H)^2 = \sum_{i=1}^{4}(g_i - h_i)^2 + (g_1 - h_1)(g_3 - h_3) + (g_2 - h_2)(g_4 - h_4), \quad (4.23)$$

this is the distance of points $G\sigma$,$H\sigma$ defined by the quadratic form

$$q(x_1, x_2, x_3, x_4) = x_1^2 + \cdots + x_4^2 + x_1x_3 + x_2x_4, \qquad (4.24)$$

which is positive definite, as is clearly seen from its definition. If $\mathbf{x} = (x_1, \ldots, x_4)$, then

$$q(\mathbf{x}) = \mathbf{x}^T \cdot G \cdot \mathbf{x}, \quad \text{with} \quad G = \begin{bmatrix} 1 & & 1/2 & \\ & 1 & & 1/2 \\ 1/2 & & 1 & \\ & 1/2 & & 1 \end{bmatrix} \qquad (4.25)$$

We define the q-norm and the q-scalar product by

$$\|\mathbf{x}\|_q = q(\mathbf{x})^{1/2}, \quad \langle \mathbf{x}, \mathbf{y} \rangle_q = \mathbf{x}^T \cdot G \cdot \mathbf{y}. \tag{4.26}$$

Remark 4.3.1. Consider a point $\mathbf{p} = (x_p, y_p, z_p)$ of the line segment $[\mathbf{g}_-, \mathbf{g}_+]$. In Equ. (4.22) we integrated its distance to the line H, which is measured within the horizontal plane $z = z_p$. The shortest distance of $\mathbf{p}$ to H differs from that distance by a factor λ with $\cos\phi \leq \lambda \leq 1$, ϕ being the angle enclosed by H and the z-axis.

If lines have the property that the angle enclosed with the z-axis does not exceed a certain value, then the distance function defined here is bounded by the Euclidean distance between lines times a certain factor.

This is in accordance with the well known property of stereographic map projections that $d(\sigma(P), \sigma(Q))/d(P, Q)$ increases if P and Q converge towards the center of the projection. ◇

Stereographic Projection of Complexes

We apply the stereographic projection σ of Equ. (4.21) to sets of lines, such as reguli $\mathcal{R}$, linear congruences $\mathcal{N}$, or linear complexes $\mathcal{C}$. Their subsets of non-horizontal lines are denoted by the symbols $\mathcal{R}^o$, $\mathcal{N}^o$, $\mathcal{C}^o$, respectively. But we will still speak of a regulus, a linear congruence, and a linear complex, even if the horizontal lines are missing.

Lemma 4.3.2. *Consider a linear complex $\mathcal{C}$ with Plücker coordinates $\mathcal{C}\gamma^\star = (\mathsf{c}, \overline{\mathsf{c}})\mathbb{R} = (c_{01} : \ldots : c_{12})$. If $\mathcal{C}$ is regular and $c_{03} \neq 0$, then $\mathcal{C}^o\sigma$ is a quadric. If $c_{03} = 0$, then $\mathcal{C}^o\sigma$ is a hyperplane. If $c_{03} \neq 0$ and $\mathcal{C}$ is a singular complex, then $\mathcal{C}^o\sigma$ is a quadratic cone. All image quadrics are homothetic, and so are all image cones.*

Proof. Equ. (4.20) shows that σ maps $\mathcal{C}^o$ to the algebraic variety with equation

$$\begin{aligned} \mathcal{C}^o\sigma: \quad & c_{03}(x_1x_4 - x_2x_3) - (c_{02} + c_{23})x_1 + (c_{01} - c_{31})x_2 \\ & + c_{23}x_3 + c_{31}x_4 + c_{12} = 0. \end{aligned} \tag{4.27}$$

This is a hyperplane if and only if $c_{03} = 0$, and a quadratic variety otherwise. Up to the scalar factor c_{03}, all possible image quadrics share the quadratic term $x_1x_4 - x_2x_3$. Two quadrics with the same quadratic terms in their equations are *homothetic*, i.e., differ from each other only by a central similarity and a translation, and so do singular quadratic varieties.

A linear complex is singular if and only if its Klein image is a quadratic cone (and therefore contains pencils of concurrent lines). This property is preserved by a central projection. This shows that regular complexes project to regular quadrics, and singular complexes to singular quadratic varieties. □

Remark 4.3.2. We projectively extend Euclidean four-space and consider the projective quadric Φ which contains $\mathcal{C}^o\sigma$. Its affine part is given by Equ. (4.27), and its equation in homogeneous coordinates $(x_0 : \ldots : x_4)$ is $c_{03}(x_1x_4 - x_2x_3) +$

$(-(c_{02}+c_{23})x_1+(c_{01}-c_{31})x_2+c_{23}x_3+c_{31}x_4+c_{12}x_0)\,x_0 = 0$. Its intersection with the ideal hyperplane $x_0 = 0$ is the quadric

$$\Psi : x_0 = x_1x_4 - x_2x_3 = 0,$$

which is independent of $\mathcal{C}$. If we look at the stereographic projection, we see why this must be so: The horizontal lines of $\mathcal{C} \setminus \mathcal{C}^o$ are those whose Klein image is contained in the tangent hyperplane of the Klein quadric at the projection center Z. They project to the quadric Ψ. Every surface tangent at Z contained in the Klein quadric appears as a projection ray, and so the ideal part of the stereographic image is the same for all linear complexes. ◇

Remark 4.3.3. The linear complexes $\mathcal{C}$ with $c_{03} = 0$ contain the horizontal line at infinity. Their Klein image contains the projection center, so the stereographic image is the hyperplane $\mathcal{C}^o\sigma : -(c_{02}+c_{23})x_1+(c_{01}-c_{31})x_2+c_{23}x_3+c_{31}x_4+c_{12} = 0$. (cf. Equ. (4.27)). ◇

Remark 4.3.4. The geometry of circles and lines in the Euclidean plane is called *Möbius geometry*. Circles may be defined as those real conics whose intersection with the ideal line has the equation $x_0 = x_1^2 + x_2^2 = 0$. It is well known (see Ex. 1.1.37 or the paragraph preceding Equ. (8.21)) that circles and lines are precisely the stereographic images of planar sections of the unit sphere in $\mathbb{R}^3$.

Analogously, those quadrics in P^4 whose intersection with the ideal hyperplane has the equation $x_0 = x_1x_4 - x_2x_3 = 0$, together with the hyperplanes of P^3, are the elements of a generalized Möbius geometry, and they are precisely the stereographic images of planar sections of the Klein quadric. ◇

Fitting a Linear Complex to Data Lines

Consider a finite number of lines L_i in Euclidean three-space and assume a Cartesian coordinate system such that no line is horizontal. Then the angles enclosed by the lines L_i and the z-axis are less or equal some value $\phi_0 < \pi/2$. A smaller ϕ_0 is better for what follows than a larger one.

We apply the transformation σ of Equ. (4.21) to L_i and get points $X_i = L_i\sigma$ with coordinate vectors $\mathbf{x}_i \in \mathbb{R}^4$. We have to fit a surface of the form (4.27) to them. One possibility to solve this problem is the following (cf. [193]): Consider the function

$$F_{\mathbf{a}}(\mathbf{x}) = a_0(x_1x_4 - x_2x_3) + a_1x_1 + \cdots + a_4x_4 + a_5,$$

where $\mathbf{a} = (a_0, \ldots, a_5)$, $\mathbf{x} = (x_1, x_2, x_3, x_4)$. We could define a 'distance' of the point $\mathbf{x}_0 \in \mathbb{R}^4$ to the surface $F_{\mathbf{a}} = 0$ by the value $|F_{\mathbf{a}}(\mathbf{x}_0)|$. However, what we actually want is to measure distances between points with the quadratic form q defined by Equ. (4.24). In order to relate these two distance functions in a neighbourhood of the surface $F_{\mathbf{a}}(\mathbf{x}) = 0$, we first consider ordinary Euclidean distance in $\mathbb{R}^4$, which has no geometric meaning in line space. The function $F_{\mathbf{a}}$ has the Taylor expansion

$$F_{\mathbf{a}}(\mathbf{x}+\mathbf{h}) = F_{\mathbf{a}}(\mathbf{x}) + \langle \operatorname{grad}_{F_{\mathbf{a}}}(\mathbf{x}), \mathbf{h}\rangle + o(\|\mathbf{h}\|). \tag{4.28}$$

The symbol $\langle\ ,\ \rangle$ denotes the ordinary Euclidean scalar product, and the symbol $o(f(\mathbf{h}))$ means a remainder term with the property that $o(f(\mathbf{h}))/\|\mathbf{h}\| \to 0$ as $\mathbf{h}$ converges towards zero.

Further, $F_{\mathbf{a}}(\mathbf{x})/\|\operatorname{grad}_{F_{\mathbf{a}}}(\mathbf{x})\|$ is a first order approximant to the distance of a point $\mathbf{x}$ to the surface $F_{\mathbf{a}} = 0$, as $\mathbf{x}$ tends towards this surface.

Let G equal the coordinate matrix of the bilinear form q (see Equ. (4.25)). We consider the q-gradient of $F_{\mathbf{a}}$, which is defined by

$$\operatorname{grad}^{(q)}_{F_{\mathbf{a}}}(\mathbf{x}) = G^{-1} \cdot \operatorname{grad}_{F_{\mathbf{a}}}(\mathbf{x}). \tag{4.29}$$

Then the Taylor expansion (4.28) is valid if we replace the scalar product, norm, and gradient, by their q-variants, as defined by (4.26). This is clear from definition of the q-gradient. Moreover, the function

$$\widetilde{F}_{\mathbf{a}}(\mathbf{x}) = F_{\mathbf{a}}(\mathbf{x})/\|\operatorname{grad}^{(q)}_{F_{\mathbf{a}}}(\mathbf{x})\|_q$$

is a first order approximant of the signed q-distance of the point $\mathbf{x}$ to the surface $F_{\mathbf{a}} = 0$. We therefore look for $\mathbf{a}$ which minimizes

$$\sum_{i=1}^{k} (\widetilde{F}_{\mathbf{a}}(\mathbf{x}_i))^2. \tag{4.30}$$

Then the surface $F_{\mathbf{a}}(\mathbf{x}) = 0$ will be a reasonable least squares fit for the data points X_i. Because the coefficients of $\mathbf{a}$ enter F in a linear way and because of the low polynomial degree of the problem this nonlinear least-squares problem is computationally tractable.

Remark 4.3.5. If the surface $F_{\mathbf{a}}(\mathbf{x}) = 0$ has a singular point $\mathbf{s}$ (this happens if the coefficient vector $\mathbf{a}$ belongs to a singular linear complex), then the vector $(\nabla_{\mathbf{x}} F_{\mathbf{a}})(\mathbf{s})$ is zero, and so data points near $\mathbf{s}$ will cause problems (such data points belong to lines near the axis of the singular complex).

The surfaces $F_{\lambda\mathbf{a}}(\mathbf{x}) = 0$ and $F_{\mathbf{a}}(\mathbf{x}) = 0$ are the same. This shows that in order to minimize the expression in (4.30) it is necessary to normalize the vector $\mathbf{a}$ in some way. The methods to solve this minimization problem are similar to those of Sec. 4.1. ◇

Fitting a Linear Congruence to Data Lines

A linear line congruence $\mathcal{N}$ is the carrier of a pencil of linear complexes. If this pencil is spanned by linear complexes $\mathcal{C}$ and $\mathcal{C}'$, then $\mathcal{N}\sigma = \mathcal{C}\sigma \cap \mathcal{C}'\sigma$. The two equations $\mathcal{C}^o\sigma : a'(x_1x_4 + x_2x_3) + \cdots$ and $\mathcal{C}'^o : a''(x_1x_4 + x_2x_3) + \cdots$ of the form (4.21) which define $\mathcal{N}^o\sigma$ have the same quadratic terms, so an appropriate linear combination is linear. We see that $\mathcal{N}\sigma$ is defined by one linear and one quadratic equation, so it is a quadric or possibly a singular quadratic variety contained

in a three-dimensional hyperplane of $\mathbb{R}^4$. Because σ preserves the linear incidence structure, it is clear that oval and ruled quadrics $\mathcal{N}\sigma$ correspond to elliptic and hyperbolic linear congruences $\mathcal{N}$, respectively. A parabolic congruence $\mathcal{N}$ is mapped to a quadratic cone, and a bundle or field of lines is mapped to a plane.

If $L_1, L_2, \ldots$ is a finite set of lines, we consider the stereographic image points $\mathbf{x}_i = L_i\sigma$. In order to fit a linear congruence to the lines L_i, we first look for a hyperplane H which contains, as best as possible, all points $\mathbf{x}_i$, where 'best' is in the sense of the metric define by the quadratic form q of Equ. (4.24). This procedure is easy and consists of an obvious modification of the same procedure in Euclidean space: Assume that H has the equation $\langle \mathbf{a}, \mathbf{x} \rangle_q + a_0 = 0$, where the q-scalar product is defined by Equ. (4.26). We minimize $\sum_i (\langle \mathbf{a}, \mathbf{x}_i \rangle_q + a_0)^2$ under the side condition that $\|\mathbf{a}\|_q = 1$. This leads to an ordinary eigenvalue problem.

Having found H, we project the points $\mathbf{x}_i$ q-orthogonally onto H. Within H, we have to approximate the points $\mathbf{x}_i$ by a quadric Q which appears as intersection of one of the quadrics of Equ. (4.27) with H. This is similar to the problem of fitting a complex to data points — the quadratic coefficients of Q's equations are already known up to a common factor.

If the best fitting quadric degenerates into a plane within H, then the original hyperplane fitting problem would have had a one-parameter family of solutions. This case can be detected by the appearance of two small solutions of the characteristic equation analogous to (4.7).

Fitting a Regulus to Data Lines

The Klein image of a linear congruence is a (possibly degenerate) quadratic variety contained in a three-dimensional subspace of P^5. A regulus is a quadratic contained in a subspace which is two-dimensional. So the problem of fitting a regulus to data lines is transformed into the problem of fitting a plane to the data points, and afterwards fitting a conic (or possibly a line) to a planar set of points. Like in the previous case, the quadratic coefficients in the conic's equation are already known up to a scalar factor. The metric used for a least squares fit is based on the quadratic form q of Equ. (4.24).

Interpolating and Approximating Real-Valued Functions of Lines

We consider the problem of *scattered data interpolation* and *approximation* for functions defined in line space. Assume that we are given a finite sequence of data lines L_i and real numbers r_i. We also define a region of interest D within line space, where the interpolant is to be defined.

We want to construct a function F which is defined on all lines L within some domain of interest, and either exactly or approximately assumes the values r_i at the lines L_i.

One possible way to solve this problem is the following [140]: Assume that a finite number of open spherical caps Γ_i cover the unit sphere, and that this covering

is symmetric with respect to the origin. A antipodal pair $+\Gamma_i, -\Gamma_i$ of caps is determined by its axis A_i of rotational symmetry and its spherical radius ρ_i. For each axis A_i, consider the set $\mathcal{L}_i \subset D$ of lines with $\sphericalangle(A_i, L) < \rho_i$.

We choose a Cartesian coordinate system such that A_i is parallel to its z-axis and consider the mapping σ of Equ. (4.21). Thus for all i we get image points $\sigma_i(L_j) \in \mathbb{R}^4$ for those data lines L_j which are contained in $\mathcal{L}_i$. It is well known how to perform scattered data interpolation and approximation in Euclidean $\mathbb{R}^4$ (cf. [78]), so we may assume that we have constructed real-valued functions F_i whose domain is $\mathbb{R}^4$ and which assume the values r_j at the points $\sigma_i(L_j)$. At last we have to glue the functions F_i together, using weight functions w_i defined on the unit sphere. Denote one of the unit vectors parallel to the line L by $\mathbf{l}(L)$. Then

$$F(L) = \sum\nolimits_i w_i(\mathbf{l}(L)) F_i(\sigma_i(L))$$

is a solution, if the weight functions w_i have the following properties: (i) $w_i(\mathbf{n}) = w_i(-\mathbf{n})$ for all $i, \mathbf{n}$ (the weights are symmetric with respect to the origin), (ii) $\sum_i w_i(\mathbf{n}) = 1$ for all $\mathbf{n}$ (the weights form a partition of unity), and (iii) w_i is zero outside $\Gamma_i \cup (-\Gamma_i)$.

Remark 4.3.6. Examples of such function are the so-called *Franke-Little weights* (cf. e.g. [9], p.112), which are defined as follows: assume that $\mathbf{a}_i$ is a unit vector parallel to the axis A_i and choose an integer $m \geq 1$. Then let

$$\begin{aligned} \widetilde{w}_i(\mathbf{n}) &= \max(|\mathbf{n} \cdot \mathbf{a}_i| / \cos\rho_i, 0)^m \\ w(\mathbf{n}) &= \sum\nolimits_i \widetilde{w}_i(\mathbf{n}) \\ w_i(\mathbf{n}) &= \widetilde{w}_i(\mathbf{n}) / w(\mathbf{n}). \end{aligned}$$

These weights are m times continuously differentiable, their support is $+\Gamma_i \cup -\Gamma_i$ by definition, and they sum up to one, also by definition. ◇

Parallel Robots

Consider a *six-legged parallel manipulator* (or parallel robot, cf. Fig. 4.5). Here a rigid body Σ (the 'moving system') is connected with another one (the 'fixed system' Σ_0) by six bars of variable length ('legs'), which have spherical links at both ends. A motion of Σ is understood as smooth family of positions $\Sigma(t)$, caused by a change in the legs' lengths.

Geometrically, we may think of the legs L_i, $i = 1, \ldots, 6$ as of lines. Special cases of such manipulators appear for example in flight simulators. They have, within bounds, the maximum degree of freedom possible, and the direct connection between the moving and the fixed system makes it possible to move heavy loads in a fast and precise manner. Research on parallel manipulators has been quite active in the past decade [123, 86]: We will show how the investigation of the mechanism's stability benefits from line geometry and from approximation methods in line space [155].

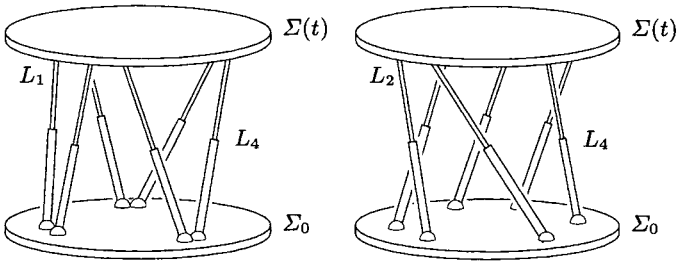

Fig. 4.5. Six-legged parallel manipulator. Left: Mechanism which is stable for all leg lengths. Right: Unstable position of another mechanism. The infinitesimal degree of freedom equals two.

Static Stability and Kinematic Stability

We consider 'mechanical structures' which consist of rigid bodies joined together by links. In statics there is the notion of *stability* of such a structure: A force acting on some point causes forces in the various joints of the structure, and if the structure is considered linearly elastic, also reversible deformations which depend linearly on these forces. An *unstable* or *singular* structure responds to exterior forces by 'infinite' induced forces — we can imagine that arbitrarily small exterior forces cause finite displacements.

Obviously if the structure admits a flexion (i.e., it is a *mechanism*), then it is unstable in this sense. A flexion consists of motions of the individual parts of the mechanical structure which are compatible with the joints.

For structures whose parts are joined by spherical links (*frameworks*), this notion of static stability is known to be equivalent to the following 'kinematic' stability.

Definition. *Assume a framework F consisting of rigid parts $K_0, \ldots, K_n$, where K_0 is assumed fixed. An infinitesimal flexion of F is an assignment of velocity vectors $\mathbf{v}(\mathbf{x})$ to all $\mathbf{x} \in F$ such that $\mathbf{v}$ is not identically zero, but is zero in K_0 and coincides with an infinitesimal motion of Euclidean space if restricted to any K_i. If F admits an infinitesimal flexion, then F is called unstable or singular, otherwise it is called stable.*

If the framework admits a smooth flexion which leaves K_0 fixed, then clearly the velocity vector field of this flexion serves as an infinitesimal flexion. It is even possible to show that a framework which admits any continuous flexion has an infinitesimal flexion, so that all flexible frameworks are singular. The following lemma is an immediate consequence of Th. 3.4.2:

Lemma 4.3.3. *A six-legged parallel manipulator is singular as a framework if and only if the legs $L_1, \ldots, L_6$ are contained in a linear line complex.*

Proof. A velocity vector $\mathbf{v}_i$ assigned to a L_i's 'moving' endpoint $\mathbf{x}_i$ fits into an infinitesimal rigid body motion of L_i leaving the other endpoint fixed if and only if

$\mathbf{v}_i \perp L_i$, and so L_i is a path normal for any infinitesimal motion of Σ. As the set of path normals is a linear complex for all infinitesimal motions, the lemma follows. □

A singular position of the parallel manipulator is one where small forces cause large displacements, which makes it e.g. unfit for use in a flight simulator. In practice it is also important to keep at a certain distance from singular positions, because the above mentioned ratio of displacement to force is not actually infinite, but too large in a whole neighbourhood of a singular position.

Snapping between Neighbouring Positions

It may happen that the parts of two different frameworks are congruent, without the frameworks themselves being congruent. We can think of a framework taken apart and rebuilt in a different way. Two such positions may be very close to each other. This situation is to be avoided in structures actually built, because it can easily happen that the framework snaps from one position to the other.

It is easy to see that a parallel manipulator which has two neighbouring positions F_1, F_2 is very close to a singular structure: Consider the endpoints $\mathbf{x}_1, \ldots, \mathbf{x}_6$ of the legs and their two position $\mathbf{x}_i^+$ and $\mathbf{x}_i^-$. Obviously there is a rigid body motion which transforms $\mathbf{x}_i^-$ to $\mathbf{x}_i^+$. According to Remark 3.1.6 the lines incident with the midpoints $\mathbf{m}_i = \frac{1}{2}(\mathbf{x}_i^+ + \mathbf{x}_i^-)$ and orthogonal to the vector $\mathbf{x}_i^+ - \mathbf{x}_i^-$ belong to a linear complex. This shows that the closer the points $\mathbf{x}_i^+, \mathbf{x}_i^-$ are, the closer is the manipulator to a singular one, and the better the legs can be fitted by a linear complex.

This can be checked with the tools shown in Sec. 4.1. Because of inavoidable imperfections of an actual structure these methods are also needed when testing for singular positions.

Degree of Singularity

If the legs are contained in a linear manifold of complexes, then its dimension plus one is called the *degree* of singularity. Degree 1 means that there is only one linear complex which the legs belong to. The methods presented in Sec. 4.1 can be used to detect such cases.

Example 4.3.2. As an example, we consider a so-called *Stewart-Gough platform* (see Fig. 4.5). Here the spherical links are arranged in two planes π of the moving and π^0 of the fixed system. We assume that the moving system moves in a translational manner such that the plane π remains constant. The legs have to vary their lengths and we get a two-parameter family of structures which is e.g. parametrized by the position of a point (u, v) within π.

Fig. 4.6 shows the deviation of the legs which belong to parameter values (u, v) to the nearest linear complex (the *stability function*). This deviation is defined by Equ. (4.3) and the nearest linear complex is found according to Lemma 4.1.2.

Computation of the stability function requires the fitting of many linear complexes to lines. This is done numerically and is reasonably fast if we have good

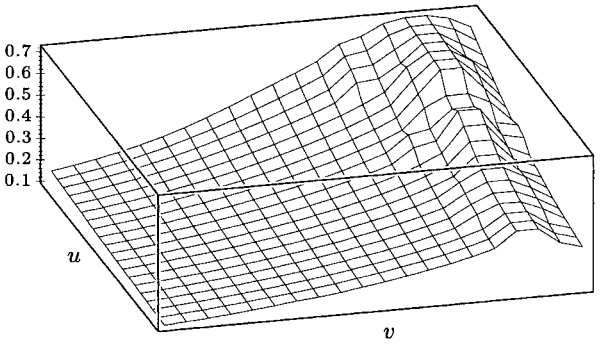

Fig. 4.6. The stability function of a six-legged parallel manipulator.

initial values for iterative algorithms — in this particular case initial values are provided by the solution complexes for neighbouring positions. ◇

Remark 4.3.7. Line geometry also plays a role in the study of singular positions of *serial* robots. For example, if the mapping of the configuration space of a $6R$ robot to the Euclidean motion group is singular, then the six rotation axes are contained in a linear complex. ◇

4.4 Approximation in the Set of Line Segments

We have already studied line segments in various places. Here we investigate briefly the set of *oriented line segments* of Euclidean 3-space E^3 and show how to solve approximation problems in it.

An *oriented line segment* $\overrightarrow{\mathbf{pq}}$ is identified with a member of $\mathbb{R}^6 = \mathbb{R}^3 \times \mathbb{R}^3$ in the obvious way:

$$(x_1, \ldots, x_6) = (p_1, p_2, p_3, q_1, q_2, q_3). \tag{4.31}$$

Oriented line segments $\overrightarrow{\mathbf{pp}}$ of zero length are identified with a *point* of Euclidean space, and are mapped to the three-dimensional diagonal subspace Δ with equation $x_1 - x_4 = x_2 - x_5 = x_3 - x_6 = 0$.

The mapping $\overrightarrow{\mathbf{pq}} \mapsto \overrightarrow{\mathbf{qp}}$ is expressed in $\mathbb{R}^6$ by $(x_1, \ldots, x_6) \mapsto (x_4, x_5, x_6, x_1, x_2, x_3)$.

Distances between Line Segments

In order to define a *distance* between two line segments $\overrightarrow{\mathbf{p}_i\mathbf{q}_i}$ $(i = 1, 2)$, we do as in (4.22) and consider a similarity transformation which maps $\mathbf{p}_1 \to \mathbf{p}_2$, $\mathbf{q}_1 \to \mathbf{q}_2$:

$$(1 - \lambda)\mathbf{p}_1 + \lambda\mathbf{q}_1 \mapsto (1 - \lambda)\mathbf{p}_2 + \lambda\mathbf{q}_2 \quad (\lambda \in [0, 1]).$$

The distance is then defined as

$$d(\overrightarrow{\mathbf{p}_1\mathbf{q}_1}, \overrightarrow{\mathbf{p}_2\mathbf{q}_2})^2 = 3\int_0^1 ((1-\lambda)(\mathbf{p}_1-\mathbf{p}_2)+\lambda(\mathbf{q}_1-\mathbf{q}_2))^2\, d\lambda \qquad (4.32)$$
$$= (\mathbf{p}_1-\mathbf{p}_2)^2+(\mathbf{q}_1-\mathbf{q}_2)^2+(\mathbf{p}_1-\mathbf{p}_2)\cdot(\mathbf{q}_1-\mathbf{q}_2).$$

Obviously this distance is simply the distance between the two points in $\mathbb{R}^6$ which correspond to the segments $\overrightarrow{\mathbf{p}_i\mathbf{q}_i}$ with respect to the quadratic form

$$q(\mathbf{x}) = x_1^2+\cdots+x_6^2+x_1x_4+x_2x_5+x_3x_6. \qquad (4.33)$$

This means that the identification of a line segment with its corresponding point in $\mathbb{R}^6$ gives us a *point model* for the set of oriented line segments, together with a distance function which is Euclidean.

Remark 4.4.1. Among the applications of this concept is approximation in line space with additional information, for instance approximation of ruled surfaces together with boundary curves (see [26]).

Approximation in line space via stereographic projection (see Sec. 4.3) is actually a special case of approximation of line segments: We assign to a line G the segments $\overrightarrow{\mathbf{g}_+\mathbf{g}_-}$ and use the distance (4.32). ◇

http://www.springer.com/978-3-642-04017-7

Computational Line Geometry
Pottmann, H.; Wallner, J.
2001, X, 564 p. 264 illus., 17 illus. in color., Softcover
ISBN: 978-3-642-04017-7